

Poloidal 2D scans to investigate potential and density profiles in the TJ-II stellarator using Heavy Ion Beam Probe

R. Sharma^{1a}, P.O. Khabanov^{2,5}, A.V. Melnikov^{2,4}, N.K. Kharchev², E. Sánchez¹, A.A. Chmyga³, G.N. Deshko³, L.G. Eliseev², C. Hidalgo¹, S.M. Khrebtov³, A.D. Komarov³, A.S. Kozachek³, L.I. Krupnik³, A. Malaquias^{1a}, B van Milligen¹, A. Molinero¹, J.L. de Pablos¹, I. Pastor¹, V.N. Zenin^{3,5} and the TJ-II team

^{1a}*IPFN, Instituto Superior Técnico, Universidade de Lisboa, 1049-001 Lisboa, Portugal.*

¹*Fusion National Laboratory, CIEMAT, 28040, Madrid, Spain*

²*National Research Centre 'Kurchatov Institute', 123182, Moscow, Russia*

³*Institute of Plasma Physics, NSC KIPT, 61108, Kharkov, Ukraine*

⁴*National Research Nuclear University MEPhI, 115409, Moscow, Russia*

⁵*Moscow Institute of Physics and Technology, 141700, Dolgoprudny, Russia*

I. Introduction

The characterization of asymmetries in plasma fluctuations is an important topic to understand and validate transport mechanisms in magnetically confined plasma fusion. The search for asymmetries in edge plasma fluctuations has shown the importance of the curvature driven instabilities in the plasma boundary region [1]. First direct experimental evidence of strong poloidal Reynolds stress asymmetry [2] also pointed out the curvature driven zonal flow, which is similar to the asymmetry observed in turbulent transport. Recent gyrokinetic simulations in stellarators show a strong localization of unstable modes along the flux surface [3, 4]. 2D core and edge density fluctuations have been previously investigated using beam emission spectroscopy [5] and fast cameras respectively [6]. 2D spatial potential profiles have been measured by heavy ion beam probe in LHD [7].

This paper reports on an attempt to experimentally characterize 2-D poloidal structures of plasma fluctuations using Heavy Ion Beam Probe (HIBP) diagnostics in the TJ-II stellarator. The experiment has allowed the investigation of 2D poloidal contour map for plasma potential and plasma density fluctuations from high to low field side.

II. Experimental set up

TJ-II has a unique experimental arrangement of a dual Heavy Ion Beam Probe (HIBP) system [8]. For this experiment both HIBPI and HIBPII were operated in scanning mode from the High to the Low Field Side (HFS to LFS). The point of ionization or sample volume probed by the injecting beam inside the plasma in a poloidal cross-section depends on the energy of primary ion beam (Cs^+) (mainly determined by injector voltage) and on the voltages on the four set of steering plates in the primary beam line to scan the beam from HFS to LFS.

Experiments were carried out in pure ECRH heated regimes ($P_{\text{ECRH}} \approx 300$ kW) with constant low density in the range $n_e \sim 0.4 \times 10^{19} \text{ m}^{-3}$ and central electron temperature $T_e \sim 1.3 - 1.6$ keV. Experiments were done for the standard magnetic configuration of TJ-II, having the edge rotational transform value close to 1.6 which corresponds to $n/m = 8/5$ rational surface located at $\rho \approx 0.8$.

HIBP-II was used for the 2D scan for the purpose of these experiments. The plasma volume scanned by HIBP moves up (vertically) by 1cm with every 2 kV increase in the injecting voltage. The injector voltage was increased from 128 to 148 kV. On top of that, for each discharge and injector voltage, the sample volume is radially scanned using the steering plates in the primary beam line. Hence, circa of $10 \times 10 \text{ cm}^2$ of the plasma volume was scanned from LFS to HFS for this experiment. The measurements for local mean and relative fluctuations in plasma density and potential are obtained using parallel plate 30° proton green energy analyser in HIBP-II [9]. The multi-slit analyser has 5 input slit that scans the 5 neighbouring plasma sample volumes simultaneously to measure plasma parameters mentioned before along with the toroidal shift (related to the poloidal magnetic field). The sampling rate of HIBP signals was 2 MHz.

Fig. 1 shows the computed point of ionization or sample volume probed (for thin beam approximation, i.e. beam diameter=0), where primary Cs^+ ions are injected with different acceleration voltages. For each injector voltage the beam is radially scanned from HFS-LFS scan in the TJ-II poloidal cross section.

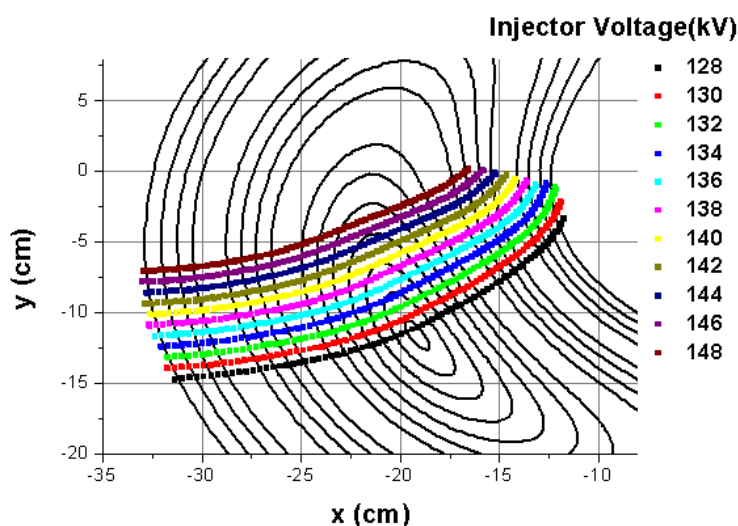


Fig.1: Plasma volume scanned in TJ-II by increasing injector voltage (increasing Cs^+ energy). For each injector voltage the beam was scanned from HFS to LFS.

III. Experimental results and discussion

Fig. 2 and 3 show 2D analysis of averaged and root mean square (rms) of fluctuations for plasma potential and secondary ion current, respectively. Results are plotted over the contour plots of magnetic flux surfaces in TJ-II.

In low density plasmas ($n \approx 0.4 \times 10^{19} \text{ m}^{-3}$) core plasma potential is positive [Fig. 2], corresponding to positive (electron root) radial electric field (E_r) in agreement with neoclassical predictions. Although, the contour plot for potential and rms of potential seems rather close to the magnetic flux surfaces, some discrepancies should be noted. The 2D map for the absolute plasma potential (Fig. 2, left) have a local maximum that is slightly shifted upwards from the axis of vacuum magnetic flux surfaces. The local maximum of rms fluctuations of potential in the range of 40 eV, is also shifted upward

(Fig. 2, right). These shifts could be accounted due to uncertainties in the primary beam trajectory calculations. In addition, up-down poloidal variation of average (in the range of 50V) and RMS values of plasma potential ($\sim 5\dots 10V$) have been observed in both LFS and HFS (Fig. 2). Whether these asymmetries represent evidence of potential asymmetries in magnetic flux surfaces as those predicted in stellarators is under investigation [10].

Fig. 3 presents the 2D poloidal map for average (left) and rms (right) values of secondary ions current (I). The secondary ion current (I) measured by HIBP is proportional to the plasma density for low plasma density regimes investigated in this experiment (due to low attenuation effects); hence, normalized level of secondary ion current fluctuations, \tilde{I}_{rms}/I , is proportional to normalised density fluctuations, \tilde{n}/n . The up-down poloidal variation in values of secondary ion current (fig. 3, left) can be accounted by instrumental effects due to variations in the primary current coupled to the primary voltage scan. Normalized rms values of secondary current fluctuations are in the range $\sim 2\dots 4\%$.

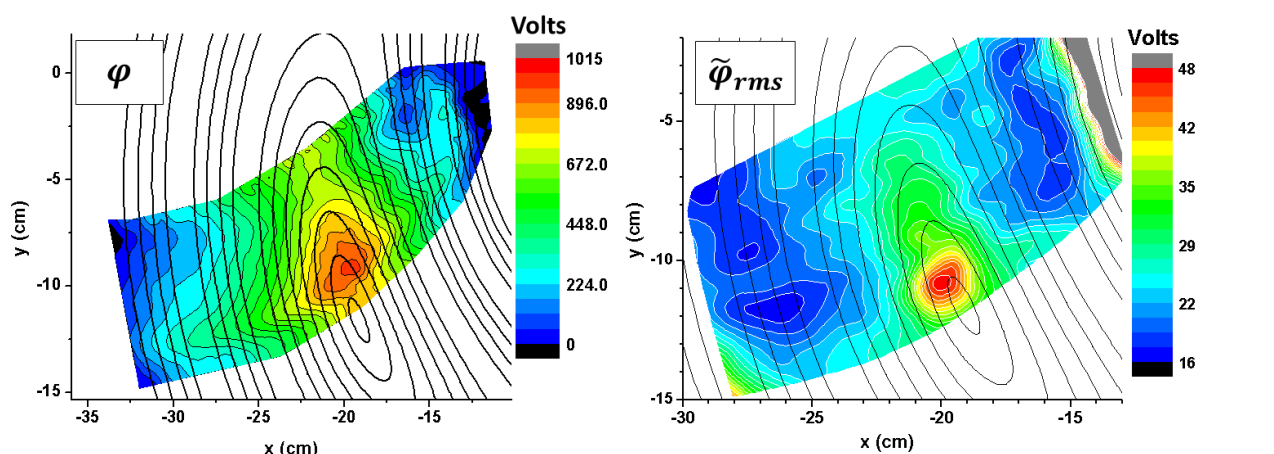


Fig. 2: 2D poloidal mapping of mean potential (left) and RMS potential fluctuations (right)

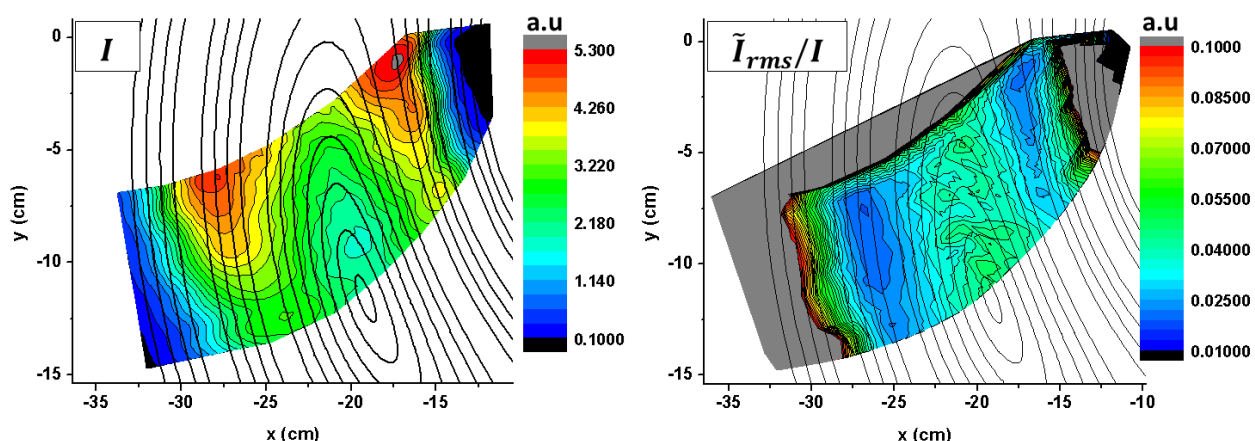


Fig. 3: 2D poloidal map for average (left) and normalized rms (right) values of secondary ion current, which is a proxy of density fluctuations

Fig. 4 (left) presents the radial profiles of the normalized level of secondary ion current fluctuations for different injector voltages. A local minimum in the fluctuations appears both in the HFS and LFS at $\rho \sim 0.6$, with LFS displaying less normalized RMS level of fluctuations than the HFS. These minima appear to be co-incident with the peaks in I profile, i.e. the transition from positive radial gradients in density profiles (fig. 4, right). These results suggest the importance of both positive and negative density gradients on plasma stability. Fluctuation levels of potential and density fluctuations are dominated by frequencies below 100 kHz.

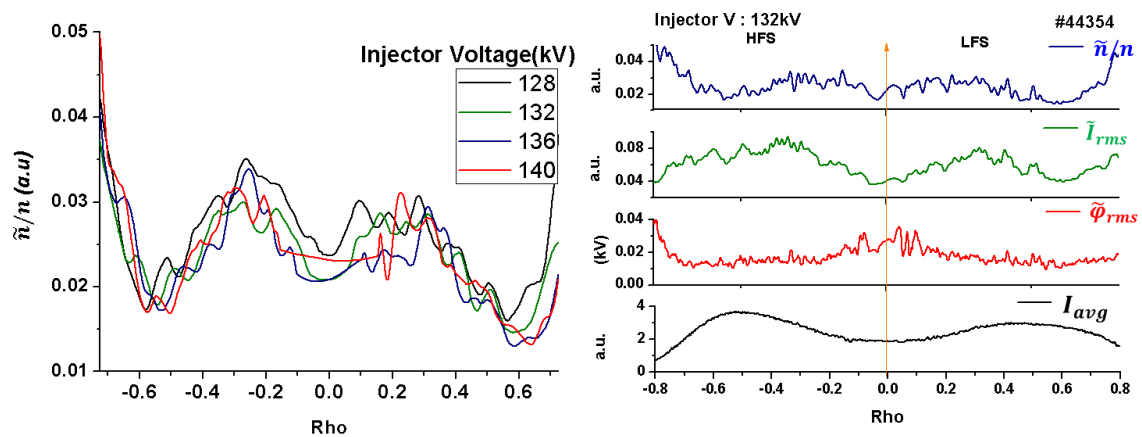


Fig. 4: Profiles of normalized rms current fluctuation level for 4 injector voltages (left); radial profiles for rms fluctuation levels in I , plasma potential and I normalized (\tilde{n}/n) value in hollow ECRH density profile. A local minima is observed in I relative fluctuations at the peaks of the I profile (right).

Future work will extend the 2-D mapping towards lower part of the plasma cross-section as well as simultaneous operation of the dual HIBP to determinate the presence of long range correlations.

The work of Kurchatov team was funded by Russian Science Foundation, project 14-22-00193. The work of AVM was partly supported by the Competitiveness Program of NRNU MEPhI. The work of Kharkov team was funded by STCU, project P-507F. IPFN activities received financial support from “Fundação para a Ciência e Tecnologia” through project UID/FIS/50010/2013. R. Sharma is supported by the Fusion DC Erasmus programme.

References

- [1] C. Hidalgo et al., Plasma Phys. Control. Fusion 37 (1995) A53
- [2] C. Hidalgo et al., Plasma Phys. Control. Fusion 59 (2017) 014051
- [3] P. Xanthopoulos et al., Physical Review X 6 (2016) 021033
- [4] E. Sánchez et al., IAEA 2018 (submitted)
- [5] Z. Yan et al., PRL 112 (2014) 125002
- [6] S J Zweben et al., Plasma Phys. Control. Fusion 49 (2007) S1
- [7] A. Shimizu et al., Review of Scientific Instruments 87 (2016) 11E731
- [8] A.V. Melnikov et al. 2017 Nucl. Fusion 57 072004
- [9] A.V. Melnikov et al., Fusion Eng.Des (2015) 10.1016/j.fusengdes.2015.01.015
- [10] J M García-Regaña et al. Nucl. Fusion, 57 (2017) 56004.